25th Congress of the European Society of Biomechanics

	TR06.6 **Cardiovascular biomechanics** Chair: D. Gallo, E. Peña **BIG HS**	TR07.2 **Cellular and sub-cellular biomechanics** Chair: G.J. Schütz, N.D. Evans **HS 03**	TR08.1 **Clinical biomechanics and computer-aided medical interventions** Chair: M.M. Morlock, L. Cristofolini **SR 06**
10:15	LAYER-SPECIFIC DAMAGE PROPERTIES OF THORACIC AND ABDOMINAL PORCINE AORTA: EXPERIMENTS AND CONSTITUTIVE MODELING J.A. Peña, M.A. Martinez, E. Peña	COMPUTER SIMULATIONS OF ELECTROMECHANICAL DRUG EFFECTS ON HUMAN STEM CELL-DERIVED CARDIAC TISSUE A. Jung, M. Goßmann, P. Linder, M. Staat	INCORPORING SUBJECT-SPECIFIC PARAMETERS IN GENERIC COMPUTATIONAL MODELS FOR ASSESSING CLINICAL OUTCOMES P. Pankaj
10:30	SYNCHROTRON-BASED PRESSURE INFLATION EXPERIMENTS TO MODEL THE MOUSE CAROTID ARTERY MICROSTRUCTURE IN 3D B. Trachet, M. Ferraro, G. Lovric, L. Aslanidou, G. Logghe, N. Stergiopulos, P. Segers	CANCER CELL MIGRATION IN CONFINED ENVIRONMENTS I. Badia-Villacampa, Y. Juste-Lanas, J.M. Garcia-Aznar, M.J. Gomez-Benito	
10:45	BIOMECHANICAL EX-VIVO RESPONSE OF ARTERIES SUBJECTED TO HYPOXIA CONDITIONS A. Navarrete, C. Garcia-Herrera, E. Herrera, B. Krause, A. Gonzalez-Candia, D. Celentano, E. Rivera	IN-SITU ANALYSIS OF TIME-DEPENDENT FORMATION ON CARTILAGE COLLAGEN STRUCTURE UNDER MECHANICAL STIMULATION K. Hamada, Y. Morita, E. Nakamachi, K. Yamamoto	3D MOTION ANALYSIS OF THE WRIST DURING DART-THROWING MOTION AFTER PARTIAL WRIST FUSION G. Fischer, L. Reissner, M. Calcagni
11:00	LOCAL IN VITRO EVALUATION OF THE BIOMECHANICAL PROPERTIES OF THE ASCENDING AORTIC ANEURYSMS S. Lin, M. Morgan, A. Lalande, A. Cochet, O. Bouchot	ANALYSIS OF SURFACE ROUGHNESS INFLUENCE DURING COLLECTIVE CELL MIGRATION T. Thenard, M. Mesnard, A. Catapano, R. Allena	COMPUTATION OF SUBTALAR JOINT CENTRE OF ROTATION IN WEIGHT-BEARING CLINICAL CT USING DVC M. Peña Fernández, D. Hoxha, G.W. Blunn, G. Tozzi, A. Goldberg
11:15	COMPUTATIONAL EVALUATION OF LONG-TERM IN-STENT RESTENOSIS BASED ON TISSUE GROWTH MODEL R. He, L. Zhao, V.V. Silberschmidt, Y. Liu	INVESTIGATING THE STRUCTURAL AND MECHANICAL PROPERTIES UNDERLYING MELANOMA TRANSITION G. Higgins, T. Abdalrahman, M.H. Zaman, J. Peres, S. Prince, T. Franz	IN SILICO MODEL-BASED PATIENT-SPECIFIC SOLUTION SYSTEM FOR BLEPHAROPTOSIS SURGERY R. Huang, R. Ogden, R. Penta, I. Gordon, S. Drummond, W. Ion
11:30	THE EFFECT OF INFLAMED ENDOTHELIAL CELL ON SHEAR-ACTIVATED PLATELETS IN ENDOVENTRICULAR THROMBOSIS F. Consolo, N. Bono, A. Dimasi, K.R. Ammann, Y. Roka Moiia, G.B. Fiore, F. Pappalardo, G. Candiani, M.J. Slepian, A. Redaelli	LOCAL MEMBRANE STRESSES AND STRAINS IN AN ERYTHROCYTE DURING INVASION BY A MALARIA MEROZOITE C. Msosa, T. Abdalrahman, T. Franz	SUBJECT-SPECIFIC HEAD MODEL DEVELOPMENT FROM A PORTABLE CONTACTLESS SENSOR FOR FACIAL MIMIC ANALYSIS AND MODELING T. Nguyen, S. Dakpé, M. Ho Ba Tho, T.T. Dao
11:45	SENSITIVITY ANALYSIS OF A THROMBECTOMY FINITE-ELEMENT MODEL THROUGH A KRIGING PROCESS G. Luraghi, S. Pant, F. Migliavacca, J.F. Rodriguez Matas	EXPERIMENTAL MECHANICS OF INDIVIDUAL COLLAGEN MOLECULES A. Rohatschek, O.G. Andriotis, P. Steinbauer, S. Baudis, C. Dworak, P.J. Thurner	IN VIVO MOTION ARTIFACTS SIGNIFICANTLY DEGRADE IMAGE REGISTRATION ACCURACY P.R. Atkins, K. Simon, L. Horling, N. Ohs, P. Christen, M. Blauth, R. Müller

SYNCHROTRON-BASED PRESSURE INFLATION EXPERIMENTS TO MODEL THE MOUSE CAROTID ARTERY MICROSTRUCTURE IN 3D

Bram Trachet (1,2), Mauro Ferraro (2), Goran Lovric (3), Lydia Aslanidou (2), Gerlinde Logghe (1), Nikolaos Stergiopulos (2), Patrick Segers (1)

1. IBiTech-bioMMeda, Ghent University, Belgium; 2. Institute for Bioengineering, EPFL, Switzerland; 3. Swiss Light Source, Paul Scherrer Institute, Villigen, Switzerland.

Introduction

The contribution of the aortic micro-structure to mechanics is still poorly understood [1]. Multiphoton imaging (MPM) has recently been used to visualize how lamellae in the mouse carotid artery react to increasing pressure [2]. However, MPM has a limited field of view and is restricted to a segment of the arterial wall. Synchrotron-based imaging could offer an alternative, but is typically used for non-pressurized, ex vivo samples. In order to overcome that limitation, we developed a synchrotron-compatible pressure inflation device that allows for quasi-static imaging of the mouse carotid artery at different pressure levels.

Methods

Six wild type (WT) and six ApoE-/- mice, all male and on a C57Bl6/J background, were used for this study. After excising the left carotid artery it was mounted on our in-house developed device. Intra-luminal pressure was increased quasi-statically from 0 to 120 mmHg with a syringe pump. At each pressure level synchrotron-based phase-propagation imaging was performed at 25m source-to-sample distance, at 25 cm sample-to-detector distance and at 21 keV. The effective voxel size was 1.625 μm^3. During the scans the axial stretch was kept at the in vivo value. For visualization purposes we skipped 2 out of every 3 axial images in the analysis, reducing the effective axial resolution to 4.9 µm and resulting in a stack of 75 images per pressure level (representing an axial length of 366 µm). The total dataset thus consisted of 8100 images (12 animals x 9 pressure levels x 75 images). Images were segmented using an in-house developed automated segmentation algorithm. Arterial diameter, length, thickness and straightness were quantified, where straightness was defined as the ratio of (i) the true lamellar length and (ii) the length of a least-square fitted circle through the lamellar data points.

Results

All three lamellar layers straightened and stretched simultaneously when intraluminal pressure was increased, confirming earlier reports [2]. In the inner lamella, lamellar length increased from 0.97 mm to 1.57 mm while the corresponding luminal diameter increased from 0.28 to 0.48 mm. This resulted in an increase in straightness from 0.89 to 0.97. The steepest increase in lamellar straightness occurred between 0 and 30 mmHg, while the lamellar length increased quasi-linearly over the entire pressure range. We did not find any statistically significant difference between WT and ApoE $^{-/-}$ mice.

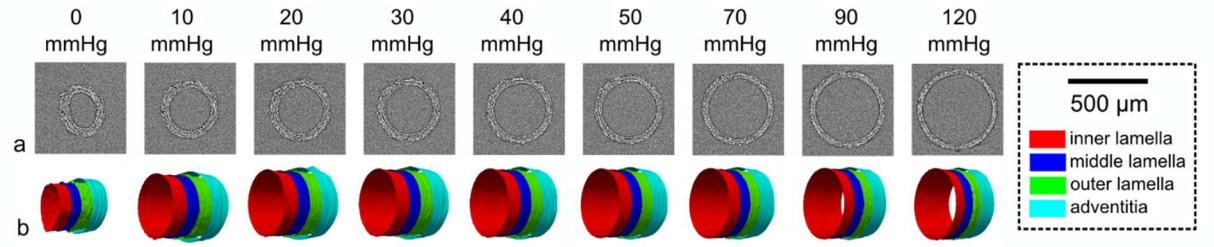

Figure 1: (a) Synchrotron images and (b) corresponding 3D segmentations of arterial lamellae and tunica adventitia in the mouse left carotid artery.

Finally, 3D models were created for each pressure level. Three lamellae and two interlamellar layers could be segmented independently. The adventitia was modelled as a homogeneous layer.

Conclusions

We present a novel methodology to visualize and segment arterial lamellae and tunica adventitia along the entire circumference of the mouse carotid artery. In a next step, the 3D models we created will form the input for computational biomechanics of the arterial micro-structure. Ultimately, we hope that such models will contribute to a better understanding of the overall mechanics of the arterial wall.

References

1.Trachet B, Aslanidou L, Piersigilli A, Fraga-Silva AR, Sordet-Dessimoz J, Villanueva-Perez P, Stampanoni M, Stergiopulos N, Segers P. Angiotensin II infusion into ApoE-/- mice: a model for aortic dissection rather than abdominal aortic aneurysm? *Cardiovasc. Res.*, 113: 1230-42, 2017.

2. Yu X, Turcotte R, Seta F, Zhang Y. Micromechanics of elastic lamellae: unravelling the role of structural inhomogeneity in multi-scale arterial mechanics. *J. R. Soc. Interface*, 15: 20180492, 2018.